Effects of silver catalyst concentration in metal assisted chemical etching of silicon

Ragavendran Venkatesan[1], Muthu Kumar Arivalagan[1], Vishnukanthan Venkatachalapathy[2,3], Joshua M. Pearce[4,5,6], Jeyanthinath Mayandi[1,*]

[1,*] Department of Materials Science, School of Chemistry, Madurai Kamaraj University, Madurai-625 021, India.

[2] Department of Physics, Centre for Materials Science and Nanotechnology, University of Oslo, PO Box 1048 Blindern, N-0316 Oslo, Norway

[3]Department of Materials Science, National Research Nuclear University "MEPhI", 31 Kashirskoe sh, Moscow, Russian Federation

[4] Department of Electronics and Nano engineering, School of Electrical Engineering, Aalto University, Espoo, Finland

[5] Department of Materials Science and Engineering, Michigan Technological University, Houghton, MI 49931, USA

[6] Department of Electrical and Computer Engineering, Michigan Technological University, Houghton, MI 49931, USA

*E-mail: jeyanthinath@yahoo.co.in

Abstract:

A systematic investigation is performed to determine the effects of the concentration of silver on metal assisted chemical etching (MaCE) for nanostructure formation mechanisms on silicon as well as their resultant optical properties. Silver nitrate concentrations of 8mM, 4mM, 3mM and 2mM with hydrogen fluoride were used for the preparation of p-type silicon nanostructures. Experimentally, it is observed that when the catalysis molarity concentration is decreased in the etching processes, it resulted in nanostructures ranging from 140 to 60 nm, respectively over the concentrations investigated. A detailed analysis of the optical properties and structure provided insight into the physics of their formation. In addition, the results show the silicon nanostructures formed black silicon where in the visible region of the spectrum the reflectance dropped by an order of magnitude. The results indicate MaCE is a promising approach to the manufacturing of antireflection coatings on black silicon-based solar photovoltaic cells. MaCE is a simple and scalable approach to enhance the optical absorption of silicon and improve the overall efficiency of the solar cell without adding significantly to the complexity, capital expenditure or cost of production.

Keywords: Metal assisted chemical etching, silver catalyst, silicon nanostructures, anti-reflection, photovoltaic

Introduction:

Silicon (Si) nanostructures have been under intense investigation for the past two decades [1] because of their potential applications in solar photovoltaics (PV) [2], thermoelectrics, energy storage, field emission, photodetectors, optical modulators and in sensing devices [3]. For example, in solar cells, the quantum efficiency determining the overall conversion efficiency is dependent on the reflection losses. Depending on the morphology, these nanostructures have the potential of improving the efficiency of solar cells, simply by improving the absorption of sunlight. Nano-texturing of Si surface (pyramids) reduces the reflectance losses in the visible region below 3% [4]. Nanostructures etched in silicon, known as "black Si" – reduce the reflection losses below 1% of all sunlight in UV and visible region against 30-10% in bare Si with anti-reflection (AR) coatings. In addition, the efficiency can be maintained with black-Si; independently of the direction of the incoming light, where conventional AR coatings are only optimized for incident light perpendicular to the cell surface [5]. Often the best results of a black silicon approach use expensive techniques such as femtosecond lasers [6], which would be challenging to scale up for mass production. Scaling is extremely important for solar photovoltaic applications, as vast areas of PV are needed to provide terawatts of power [7] needed for a sustainable global energy supply [8]. The preparation of low-cost black silicon is particularly promising in solar photovoltaic (PV) applications [9-12]. Already black Si PV with interdigitated back-contacts has achieved over 22.1% efficiency with ALD passivation of a more expensive method (cryogenic deep reactive ion etching) of fabricating silicon nanostructures [13]. Amongst various methods used for fabrication of silicon nanostructures [14], metal assisted chemical etching (MaCE) is one of the simplest and least expensive [15]. With MaCE previously deposited noble metal layers or particles act as catalysts for oxidant reduction in the etching solution and provides the required hole-current for silicon dissolution [16]. Preferred metal catalysts are silver, gold, platinum and palladium [3, 17] deposited by various techniques such as sputtering, evaporation, electrochemical [18] etc. The metal is deposited as spatially separated nano-clusters or as a continuous metal layer depending on the deposition method. After metal deposition, a solution containing hydrofluoric acid and an oxidizing agent such as hydrogen peroxide or nitric acid etches the silicon [16]. Although a theoretical model of etching exists for both continuous [19] and locally distributed [15] metal catalysts on silicon, the influence of the metal concentration on the etching process has not been well investigated. Importantly, the wettability of the Si surface is known to vary with surface morphology, time and ambient conditions [20].

To begin to fill in this scientific knowledge gap, this study the process flow of nanostructure formation by varying the catalysis concentration (by varying the diluent concentration) on the silicon substrate through MaCE is illustrated. The resultant nanostructured Si was characterized both microstructurally and optically to provide further insight into the physics of the nano silicon formation, as well as evaluate them for applications in solar photovoltaic devices.

2. Method:

Double sided polished p-type electronic grade 525 μm thick silicon wafers (100) with 1-10 Ω-cm resistivity, were used for the etching process. The silicon wafers were subjected to Radio Corporation of America (RCA) cleaning process and then cleaved to produce 1 cm x 1 cm samples. A uniform protective oxide layer was formed using a piranha solution of

sulphuric acid and hydrogen peroxide (H_2SO_4:H_2O_2) [3] in a volume ratio of 3:1 at 0^oC for 10 minutes. Before the etching process, the oxide layer was removed by dipping the sample in a water and hydrogen fluoride (H_2O: HF) solution with the volume ratio of 10:1 for 3 minutes at room temperature. Then, the silver nanoparticles (Ag NPs) were coated on the freshly cleaned Si wafers by immersing in a bath solution containing 3.6 ml of HF (40%) and 20 ml of silver nitrate (containing 28 mg of $AgNO_3$) aqueous solution for one minute. The excess Ag^+ ions present in the surface were washed with distilled water, then samples were immersed in etching solution comprising 3.6 ml of HF (48%) in 20 ml of H_2O and 0.6 ml of H_2O_2 (50%) for 45 minutes. The different concentrations with molar ratios 8mM, 4mM, 3mM and 2mM of $AgNO_3$ by varying the diluent volume (28mg $AgNO_3$ in 20 ml, 40 ml, 60 ml and 80ml of water, respectively) were used for the preparation of Si nanostructures with a constant etching time (1 minute) and are labelled as 8mM, 4mM, 3mM & 2mM respectively. The residual Ag NPs on the sample surface and in the pores of the Si were removed by immersing the samples in diluted nitric acid (H_2O:HNO_3 69%) (3:1) for 60 minutes. Finally, the prepared samples were washed with distilled water and dried in nitrogen (N_2).

The as-prepared samples were characterized using scanning electron microscopy (SEM) to analyse the morphology of the silicon nanostructures. The reflectance properties of the silicon nanostructures were measured in a range from 300 nm to 800 nm using a JASCO (V 650) UV-Vis spectrometer.

3. Results and Discussion:

3.1. SEM:

Figure 1 displays SEM micrographs of the silver (Ag) nanoparticles on the Si surface with various concentrations. The white spots on the SEM image are Ag nanoparticle randomly distributed on the silicon surface. The respective histogram is shown as the inset in Fig. 1. As can be seen by Fig. 1, as the molar concentration of the $AgNO_3$ solution decreases the size of the Ag island-NPs decreases and the surface coverage increases. In addition, it should be noted that a very thin continuous Ag layer in addition to Ag islands is formed on the Si surface except for 4mM sample, where only isolated Ag islands are present. Similar observations were made during time-dependant deposition palladium (Pd) [3] and Ag [17] metal nanoparticles on Si substrate. Increase in surface coverage and Pd (electrochemical) & Ag (sputtering) formation on Si surface was correlated to contact angle and wetting properties with respect to the deposition time. However, in the present work, the deposition time is kept constant; decrease in $AgNO_3$ solution molar concentration increases the diluent (H_2O) concentration modifying the wetting properties of the Si surface [20,21]. The Ag nuclei attached to the Si substrate have higher electronic activity than silicon atoms, which makes the reaction to occur constantly and results in the Ag nuclei gradually growing up to form Ag NPs [22]. Increasing the wettability of the Si surface increases the Ag nuclei distribution.

Figure 2 shows the top-view SEM images at 7kX and 20kX of the as-prepared Si nanostructured arrays with different molar concentrations of $AgNO_3$ solution. Comparing the top views of silicon nanostructures, the surface density increases with increase of $AgNO_3$ solution molar concentration as would be expected. Thus, the size of the voids in the 8mM sample (a) is larger than the other samples, because of the larger size of the Ag NPs, since Ag metal acts as the catalyst and reactive site for the etching of Si [23]. It should also note that the surface morphology of 3mM and 2mM sample appears to be porous in nature and exhibits

very rough surface. This could be attributed to the decrease in Ag NPs size and increase in surface coverage.

For a clearer understanding of the morphology of the Si nanostructures, Fig. 3 shows a typical cross-sectional SEM image of 8mM and 4mM samples. For 4mM sample, one can observe that silicon nanostructures look like quasi-ordered nano-grass with preferential orientation along the [100] crystallographic direction. This indicates that the MACE of *c*-Si in HF-solution is strongly crystallographic oriented, which is in agreement with results of past studies [24, 25]. While the thickness (diameter size) of silicon nanostructures is variable (about 60 to 140 nm) in the form of an array, for each individual silicon nanostructure the diameter does not vary significantly along the length. Importantly, the surface remains flat for 4mM, while 8mM sample exhibits rough surface and the nanostructures appear random near the surface. In addition, deep etched structures could also be observed with random distribution. Similar observations were made for 3mM and 2mM sample; however, the deep etched structures etch depth and randomness decreases. The 8mM sample has less surface coverage and large Ag NPs along with uniform coverage of Ag on Si surface. The random deep etches observed in 8mM could be correlated with larger Ag NPs on the Si surface. The 4mM sample exhibited isolated islands and hence resulted in formation of nanowire structures. On the other hand, the surface coverage increased for 3mM and 2mM causing random nanostructures and surface roughness increases with porous nature. Raj Kumar et.al, explored the influence of Si oxidation rate on the size of Ag catalyst. In addition, tuneable morphologies from irregular porous to regular nanowire structure were demonstrated by controlling the size of Ag NPs and H_2O_2 concentration [15]. Since the concentrations of HF and H_2O_2 are constant in this experiment, the etching characteristics will depend on the surface coverage and Ag NPs size.

The surface coverage of Ag NPs on the silicon surface influences the surface density of the silicon nanowire arrays rather than the length. The length of silicon nanostructures is controlled by duration of the etching catalysed by Ag NPs or by size of the Ag NPs [26]. Less intuitively, the linear variations of the normalized etch rate of silicon nanostructures depends on the surface coverage and size of Ag NPs. This is a result of the process of HF diffusion toward the Ag NP/Si interface to dissolve oxidized Si surface atoms after hole injection from the Ag NPs. For the higher concentrations the time needed for the HF to diffuse the oxidized Si is longer. The etch rate is affected by the "free" area between Ag NPs, in the sense that the etching rate decreases when Ag NPs get closer. Summarizing, larger Ag NPs mediate high etch rates compared to small NPs and high H_2O_2 concentration breaks down the larger Ag NPs into smaller NPs forming random nanostructures during etching process. In this work, the duration of etching and H_2O_2 concentration are kept constant, thus the length of the silicon nanostructures is constant at around 9 μm for 4mM sample, where the Si surface was covered with isolated Ag NPs. However, irregular porous with random deep etch with 10-13 μm length occurs due to breaking down of larger Ag NPs in the case of 8mM sample. High surface coverage of Ag NPs on the Si surface increases the porous nature of the 3mM and 2mM sample. In this work, it is assumed that the normalization allows to roughly take into account the influence of the distance between Ag NPs on etch rates, with the exception of the sample with the lowest coverage and smallest NP size. This is because the increase of the etching depth resulted in a lower probability for HF to access the interface [24]. Finally, the silver contamination at the bottom of the etch pits in the silicon nanostructures can be easily removed by treating the etched Si samples in HNO_3 solution.

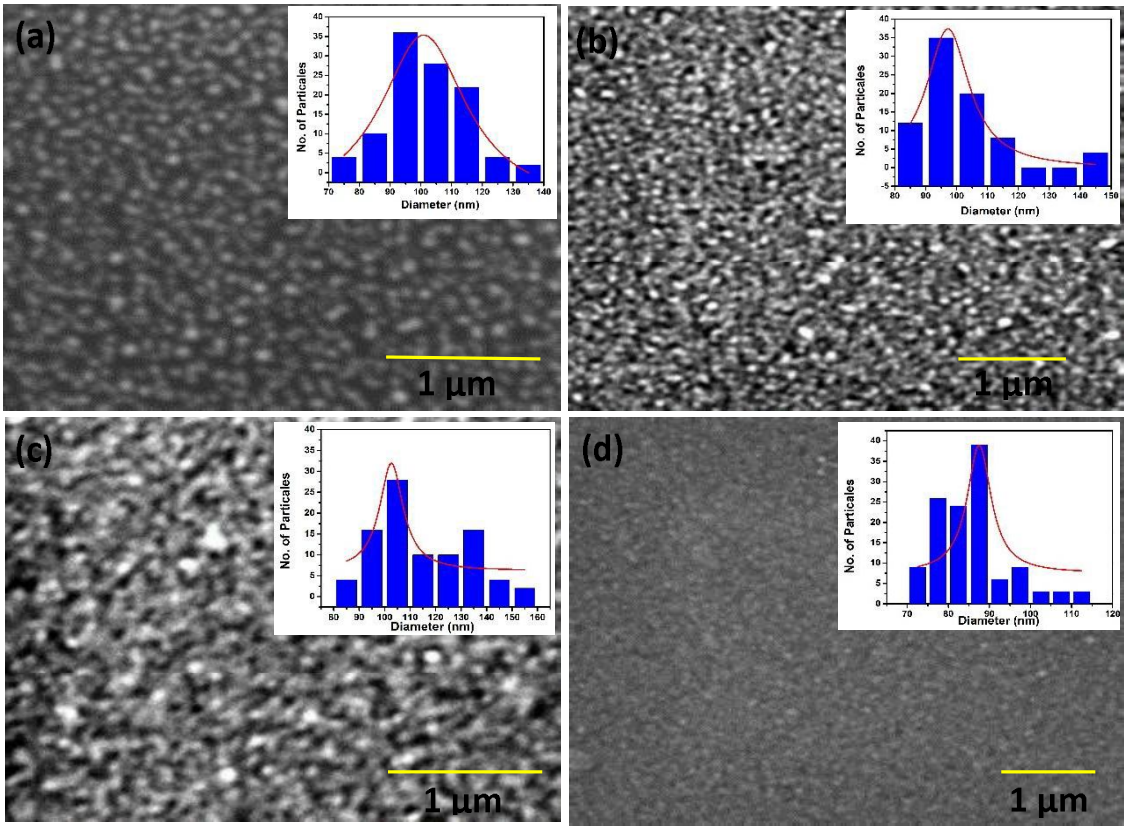

Fig. 1: SEM images of Ag NPs on silicon for various molar concentrations of $AgNO_3$ solution: (a) 8mM, (b) 4mM, (c) 3mM & (d) 2mM. The distribution of the particle size is shown in the inset of each image and the average particle size for (a) 110 ± 20 nm, (b) 100 ± 10 nm, (c) 90 ± 20 nm, (d) 80 ± 15 nm. For all $AgNO_3$ concentrations metal clusters show logarithmic-normal distributions.

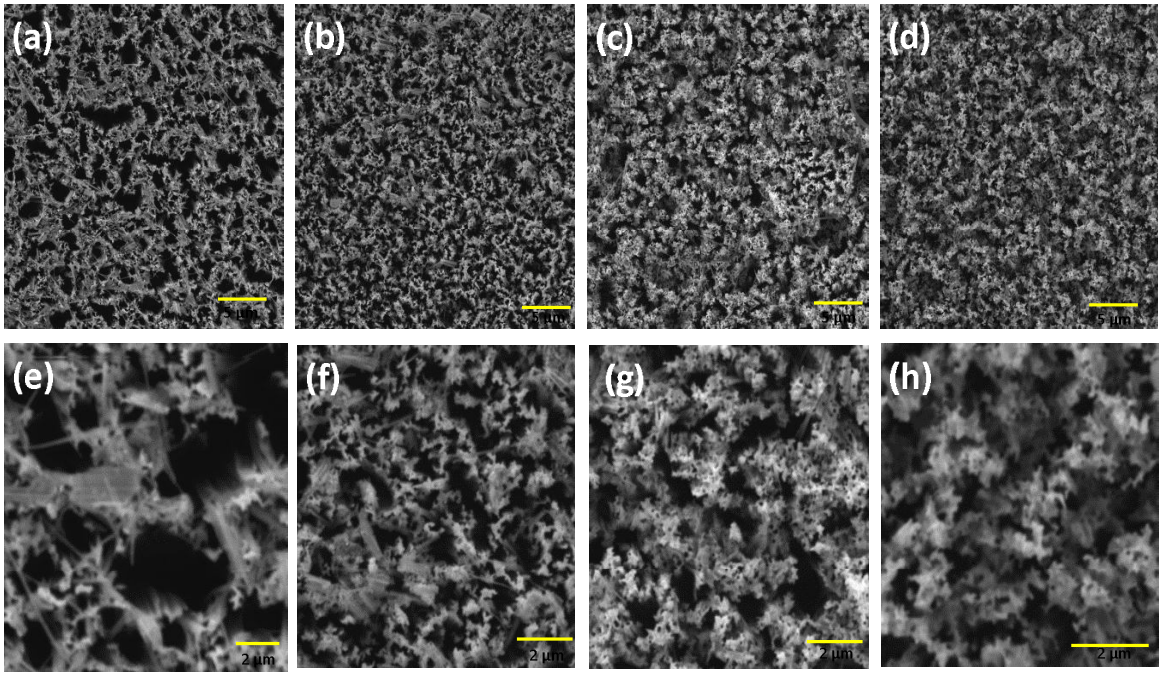

Fig. 2: SEM images of nanostructured Si for various concentration of $AgNO_3$ solution (a,e) 8mM, (b,f) 4mM, (c,g) 3mM, & (d,h) 2mM samples with different magnification.

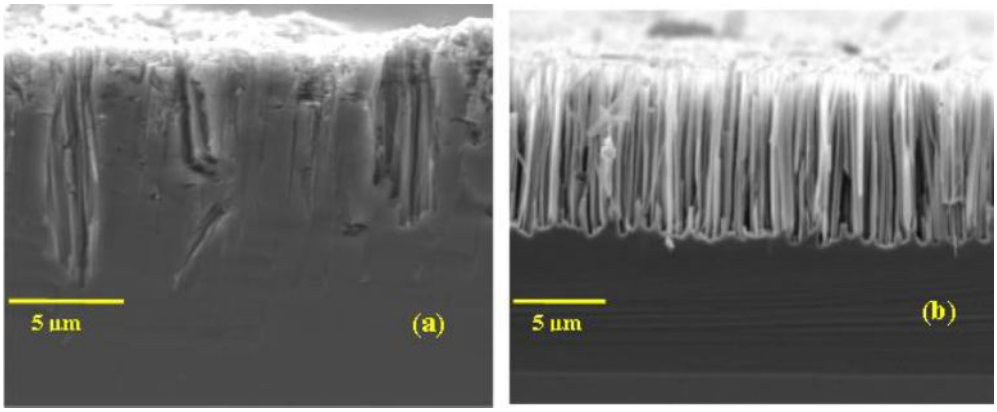

Fig. 3: Cross sectional SEM images of nanostructured Si for sample (a) 8mM & (b) 4mM of $AgNO_3$ solution.

3.2. UV- Visible Spectroscopy

The optical properties of the prepared Si nanostructures were studied using diffuse surface reflectance method. Figure 4 shows the reflectance spectra for nanostructured Si fabricated using various molar concentration of $AgNO_3$ solution. The measured reflectance of the silicon nanostructures for 8mM sample varies from 24 % in longer wavelengths (800 nm) and gradually decreases to below 7 % at shorter wavelengths (300 nm). On the other hand, the polished reference Si surface has reflectance between 48 – 27 % in the UV and visible region. The reflectance is low across the entire absorption spectrum making it an especially viable candidate for reducing reflection losses in silicon-based solar photovoltaic cells. The average surface reflectance of the Si substrate in the measured range decreased dramatically from 50% for the Si reference to less than 5% in the lower wave length region for sample 4mM sample with nanowire structure. Nishijima et.al [4], demonstrated high aspect ratio nanowire structure to have reduced reflection losses (< 0.3%) throughout the UV-visible wavelength range. Importantly, the quantum efficiency drops drastically near the UV region for the Si solar cell with pyramid structures and anti-reflection coating because of high reflectance (3-10%). In the present work, all the etched Si samples except 2mM sample, exhibit reflectance < 5% in 300 -400 nm wavelength.

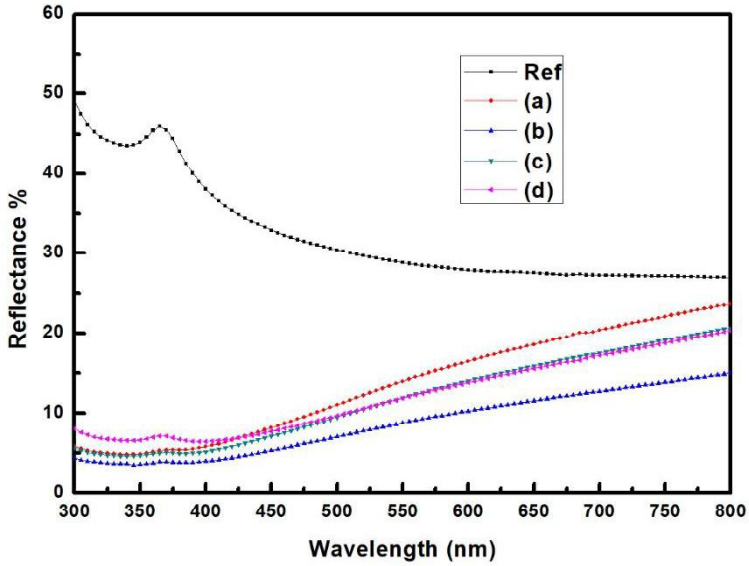

Fig. 4: UV–visible reflectance spectra of nanostructured Si for various molar concentrations of $AgNO_3$ solution (a) 8mM, (b) 4mM, (c) 3mM & (d) 2mM

Conclusions:

From the observed SEM results, the morphological properties of silicon nanostructures fabricated with MaCE process by varying the catalyst molar concentration were investigated. The depth of the different silicon nanostructures was revealed by cross sectional SEM. The etching process of silicon nanostructures were discussed based on the observed SEM results. The optical characterization results, indicated that MaCE is a promising technique for fabricating black Si, where the reflectance dropped to 5% in the UV region and 6-20% in the visible region. The results of this approach make MaCE a promising technically viable candidate for an antireflection coating system of black silicon solar photovoltaic cells. MaCE is a of simple, wet-chemical, and scalable approach to enhance the optical absorption of Si and improve the overall efficiency of the solar cell without adding significantly to the complexity, capital expenditure or cost of production.

Disclosures:

The authors declare no competing financial interests.

Acknowledgement:

The authors are thankful to the support from DST-SERB/F/1829/2012-2013, Fulbright Finland, and DST – PURSE programme MK University, for providing the SEM facility.

References:

[1] A.G. Cullis, L.T. Canham, P.D.J. Calcott, The structural and luminescence properties of porous silicon, J. Appl. Phys. 82 (1997) 909-965.

[2] C.H. Foslia, A. Thøgersen, S. Karazhanov, E.S. Marstein, Plasmonics for Light Trapping in Silicon Solar Cells, Energy Procedia 10 (2011) 287-291.

[3] J. Chen, C. Chen, C. Wong, C. Chen, Inherent formation of porous p-type Si nanowires using palladium-assisted chemical etching, Appl. Surf. Sci. 392 (2017) 498-502.

[4] Y. Nishijima, R. Komatsu, S. Ota, G. Seniutinas, A. Balčytis, S. Juodkazis, APL Photonics 1 (2016) 076104.

[5] H. Savin, P. Repo, G. van Gastrow, P. Ortega, E. Calle, M. Garín, R. Alcubilla, Nat. Nanotechnol. 10 (2015) 624-628.

[6] T. Sarnet, M. Halbwax, R. Torres, P. Delaporte, M. Sentis, S. Martinuzzi. S. Bastide, Femtosecond laser for black silicon and photovoltaic cells, In Proc. SPIE 6881 (2008) 688119.

[7] P.C. Vesborg, T.F. Jaramillo, Addressing the terawatt challenge: scalability in the supply of chemical elements for renewable energy, RSC Adv. 21 (2012) 7933-7947.

[8] J.M. Pearce, Photovoltaics - a path to sustainable futures, Futures 34 (2002) 663-674.

[9] J.S. Yoo, I.O. Parm, U. Gangopadhyay, K. Kim, S.K. Dhungel, D. Mangalaraj, J. Yi, Black silicon layer formation for application in solar cells, Sol. Energy Mater. Sol. Cells 90 (2006) 3085-3093.

[10] S. Koynov, M.S. Brandt, M. Stutzmann, Black nonreflecting silicon surfaces for solar cells, Appl. Phys. Lett. 88 (2006) 203107.

[11] H.C. Yuan, V.E. Yost, M.R. Page, P. Stradins, D.L. Meier, H.M. Branz, Efficient black silicon solar cell with a density-graded nanoporous surface: optical properties, performance limitations, and design rules, Appl. Phys. Lett. 95 (2009) 123501.

[12] J. Oh, H.C. Yuan, H.M. Yuan, An 18.2%-efficient black-silicon solar cell achieved through control of carrier recombination in nanostructures, Nat. nanotechnol. 11 (2012) 743-748.
[13] K. Tsujino, M. Matsumura, Texturization of multicrystalline silicon wafers for solar cells by chemical treatment using metallic catalyst, Sol. Energy Mater. Sol. Cells 90 (2006) 100-110.
[14] J. Cichoszewski, M. Reuter, F. Schwerdt, J.H. Werner, Role of catalyst concentration on metal assisted chemical etching of silicon, Electrochim. Acta, 109 (2013) 333- 339.
[15] Z. Huang, N. Geyer, P. Werner, J. de Boor, U. Gösele, Metal-Assisted Chemical Etching of Silicon: A Review, Adv. Mater. 23 (2011) 285-308.
[16] P. Dutheil, A.L. Thomann, T. Lecas, P. Brault, M. Vayerb, Sputtered Ag thin films with modified morphologies: Influence on wetting property, Appl. Surf. Sci. 347 (2015) 101-108.
[17] C. Yang, Y.J. Zhao, L.M. Kang, D.D. Li, W.W. Zhang, L.C. Zhang High-strength silicon brass manufactured by selective laser melting, Mater. Lett. 210 (2018) 169-172
[18] N. Geyer, B. Fuhrmann, Z. Huang , J. de Boor , H.S. Leipner , P. Werner, Model for the Mass Transport during Metal-Assisted Chemical Etching with Contiguous Metal Films as Catalysts, Phys. Chem. C 116 (2012) 13446-13451.
[19] E.C. Muñoz, C. Díaz, E. Navarrete, R. Henríquez, R. Schrebler, R. Córdova, R. Marotti C. Heyser, Characterization of Surface Changes on Silicon and Porous Silicon after Interaction with Hydroxyl Radicals, Arab. J. Chem. (2017), DOI: 10.1016/j.arabjc.2016.11.008.
[20] M. Barisik, A. Beskok, Wetting characterisation of silicon (1,0,0) surface, Mol. Simulat. 39 (2013) 700-709.
[21] Y. Liu, G. Ji, J. Wang, X. Liang, Z. Zuo and Y. Shi, Fabrication and photocatalytic properties of silicon nanowires by metal-assisted chemical etching: effect of H_2O_2 concentration, Nanoscale Res. Lett. 7 (2012) 663.
[22] J. von Behren, L. Tsybeskov, and P. M. Fauchet, Preparation and characterization of ultrathin porous silicon films, Appl. Phys. Lett., 66 (1995) 13, 1662-1664.
[23] R. J. M. Fonseca, J. M. Saurel, A. Foucaran, J. Camassel, E. Massone, T. Taliercio, and Y. Boumaiza, Acoustic investigation of porous silicon layers, J. Mater. Sci. 30 (1995) 35-39.
[24] K. Rajkumar, R. Pandian, A. Sankarakumar, R. T.R. Kumar, Engineering Silicon to Porous Silicon and Silicon Nanowires by Metal-Assisted Chemical Etching: Role of Ag Size and Electron Scavenging Rate on Morphology Control and Mechanism, ACS Omega 2 (2017) 4540-4547.
[25] R. Ouertani, A. Hamdi, C. Amri, M. Khalifa, H. Ezzaouia, Formation of silicon nanowire packed films from metallurgical-grade silicon powder using a two-step metal-assisted chemical etching method, Nanoscale Res. Lett. 9 (2014) 574.
[26] S.D. Hutagalung, M.M. Fadhali, R.A. Areshi, F.D. Tan, Optical and Electrical Characteristics of Silicon Nanowires Prepared by Electroless Etching, Nanoscale Res. Lett. 12 (2017) 425.